

# Towards the use of X-ray Free-Electron Laser electron beams to study Quantum Chromo-Dynamics

Eugene Bulyak\*

National Science Center ‘Kharkiv Institute of Physics and Technology’, 1 Academichna str, Kharkiv, Ukraine  
V.N. Karazin National University, 4 Svobody sq., Kharkiv, Ukraine

(LUXE Collaboration)

Svitozar Serkez† and Gianluca Aldo Geloni

European XFEL, Holzkoppel 4, 22869 Schenefeld, Germany

(Dated: September 28, 2023)

X-ray free-electron lasers (XFELs) utilize high-density and high-energy electron bunches which are well-suited to produce Compton back-scattering radiation. Here we study back-scattered radiation pulses produced by the interaction of XFEL electron beams and an optical laser. We discuss cost-effective setups to study such processes, taking advantage of the existing conventional as well as proposed XFEL infrastructure. We estimate parameters of possible experiments and compare them with other projects under construction.

## I. INTRODUCTION

The purpose of X-Ray Free-Electron Lasers (XFEL) is to generate extremely brilliant, ultra-short and almost spatially coherent pulses of X-rays at wavelengths down to the order of  $1 \text{ \AA}$ , in order to exploit them for scientific experiments in a variety of disciplines spanning physics, chemistry, materials science and biology, [1].

However, the electron beams of XFELs possess unique characteristics in energy and phase-space density, which may also be applied for experiments in other areas of physics. In particular, if these beams collide with intense pulses of quasi-monochromatic polarized photons, scattered high-energy polarized gamma-ray photons are produced, which are extremely useful for particle physics experiments and, in particular, Quantum Chromo-Dynamics (QCD).

Multi-GeV gamma-ray photons are useful tools in the investigation of the structures and properties of hadrons via their interaction with a target nucleon or nucleus. In particular, they are suitable for hadron studies in the strange sector. The search for QCD exotics uses data from a wide range of experiments and production mechanisms. A few of such setups are currently under construction, see [3, 4]. These setups do not cover the gamma energy range of 2.89–8.4 GeV.

Here we propose to employ the electron beams from the European XFEL accelerator to produce Compton back-scattered radiation pulses of polarized gamma-ray photons with the maximum energy of up to 4 GeV for QCD experiments.

After this introduction, the second section of this paper briefly surveys properties of Compton back-scattering radiation with emphasis on gamma-rays production. The third section presents a schematic setup of a Compton

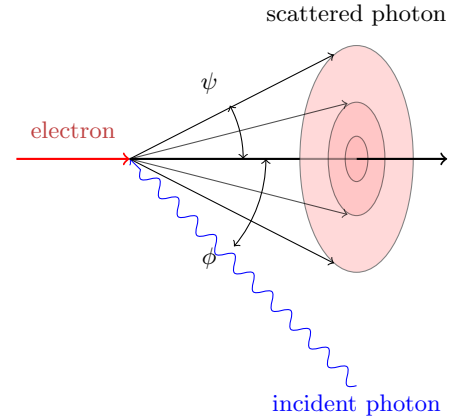


FIG. 1. Scheme of scattering the laser pulse.

source based on the European XFEL electron beam to provide capabilities for QCD experiments with photons in the multi-GeV energy range. Finally, the paper is concluded with a summary.

## II. COMPTON BACK-SCATTERING PROCESS AT HIGH ELECTRON ENERGY

Compton scattering, at variance with the classical Thomson process with low energy incident photons in the electron rest frame, exhibits modification of the spectra and angular distribution of the scattered photons due to recoil of the electrons.

A scheme of Compton back-scattering process is presented in Fig. 1.

Usually, Compton backscattered photons are referred to as quasi-monochromatic. In fact, due to the strong correlation between the scattering angle  $\psi$  and the photon energy, proper collimation enables one to select a well-defined energy range.

\* bulyak@kipt.kharkov.ua, eugene.bulyak@desy.de

† svitozar.serkez@xfel.eu

### A. Kinematics

The relation between the energy of a gamma-ray photon and the angle of emission determined from kinematics – the energy-momentum conservation law – reads (see, e.g., [5, 6]):

$$\omega \approx \frac{2\gamma_*^2(1 + \cos \phi)\omega_{\text{las}}}{1 + \gamma_*^2\psi^2}; \quad (1)$$

$$\gamma_* := \frac{\gamma}{\sqrt{1 + 2(1 + \cos \phi)\gamma\omega_{\text{las}}}}, \quad (2)$$

where  $\omega$  is the energy of the scattered quanta,  $\omega_{\text{las}}$  is the energy of laser photons,  $\gamma$  is the energy of electrons,  $\phi$  and  $\psi \ll 1$  are the crossing angle and the scattering angle of photons, see Fig. 1.

Here we make use the natural system of units for particle and atomic physics,  $\hbar = c = m_e = 1$ . Therefore  $\gamma := E_e/m_e c^2$  is the Lorentz-factor of electrons,  $\omega := \epsilon/m_e c^2$  equivalent Lorentz-factor of the scattered photons of energy  $\epsilon$ ,  $\omega_{\text{las}} := \hbar\omega_{\text{las}}/m_e c^2$  the equivalent Lorentz factor for the laser photons.

The energy of the recoiled electron becomes

$$\gamma' = \gamma - \omega = \gamma \left( \frac{1 + \gamma^2\psi^2}{1 + 2\gamma\omega_{\text{las}}(1 + \cos \phi)} \right),$$

and the energy of laser photon in the electron rest frame, see [7, 8] is

$$\eta = (1 + \cos \phi)\gamma\omega_{\text{las}} \approx 2\gamma\omega_{\text{las}}. \quad (3)$$

Under the assumption of small angles,  $\phi \ll 1, \psi \ll 1$ , Eq. (1) yields a simple expression for the maximum energy of the scattered quanta:

$$\omega^{\text{max}} = \gamma \frac{4\gamma\omega_{\text{las}}}{1 + 4\gamma\omega_{\text{las}}}, \quad (4)$$

which reveals that the recoil effect is governed by the term  $4\gamma\omega_{\text{las}} = 2\eta$ . For relatively weak electron recoil,  $4\gamma\omega_{\text{las}} \ll 1$ , the maximum energy of the scattered photons scales linearly with the laser photon energy and quadratically with the electron energy,

$$\omega \approx 4\gamma^2\omega_{\text{las}},$$

as illustrated in Fig. 2 that is computed for the energy range of the European XFEL accelerator and laser photons with an energy of 1 eV.

Accordingly, the *minimal energy* of recoiled electron is

$$\gamma'_{\text{min}} = \frac{\gamma}{1 + 4\gamma\omega_{\text{las}}}.$$

Another parameter deduced from kinematics is the angle (measured from the incident electron trajectory) at which scattered photons possess the half-maximum energy,  $\omega_{1/2} = \omega_{\text{max}}/2$ :

$$\psi_{1/2} = \frac{\sqrt{1 + 2\gamma\omega_{\text{las}}(1 + \cos \phi)}}{\gamma} = \frac{1}{\gamma_*}. \quad (5)$$

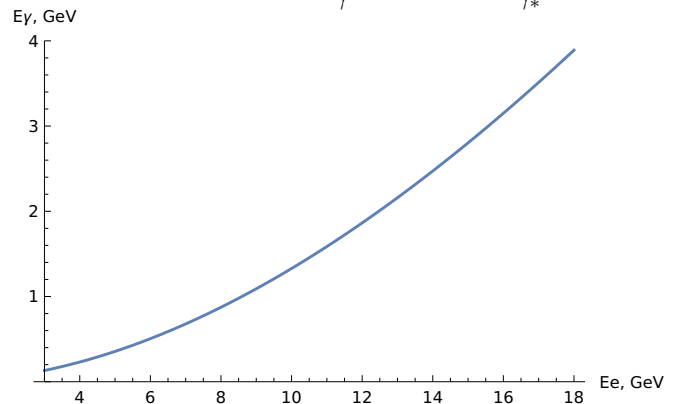


FIG. 2. Maximum energy of back-scattered gammas vs. energy of electrons.

In the low-energy Thomson's limit,  $\gamma_* \approx \gamma$ , and the energy of gamma-rays drops by half at the emission angle of  $1/\gamma$ . In the electron rest frame it corresponds to the scenario when a photon scatters perpendicularly to the incident direction.

### B. Spectrum and cross-section

A high-energy approximation for the Klein-Nishina formula was derived by Arutyunian and Tumanian [9] (see also [10]). One has the following dependence of the cross section on the frequency of the scattered photons:

$$\frac{d\sigma_{\text{Com}}}{d\omega} = \frac{3\sigma_{\text{Th}}}{16\gamma^2\omega_{\text{las}}} \left[ \frac{\omega^2}{4\gamma^2\omega_{\text{las}}^2(\gamma - \omega)^2} - \frac{\omega}{\gamma\omega_{\text{las}}(\gamma - \omega)} + \frac{\gamma - \omega}{\gamma} + \frac{\gamma}{\gamma - \omega} \right] \Theta \left( \frac{4\omega_{\text{las}}\gamma^2}{4\omega_{\text{las}}\gamma + 1} - \omega \right), \quad (6)$$

while the integral is

$$\sigma_{\text{Com}} = \frac{3\sigma_{\text{Th}}}{32\gamma^3\omega_{\text{las}}^3} \left\{ \frac{4\gamma\omega_{\text{las}}(2\gamma\omega_{\text{las}}(\gamma\omega_{\text{las}} + 4)(2\gamma\omega + 1) + 1)}{(4\gamma\omega_{\text{las}} + 1)^2} + [2\gamma\omega_{\text{las}}\gamma\omega_{\text{las}} - 1] \log(4\gamma\omega_{\text{las}} + 1) \right\}, \quad (7)$$

where  $\sigma_{\text{Th}} = 8\pi r_0^2/3$  is the Thomson cross section ( $r_0$  the classical electron radius),  $\Theta(\cdot)$  is the Heaviside's Theta function (unit step).

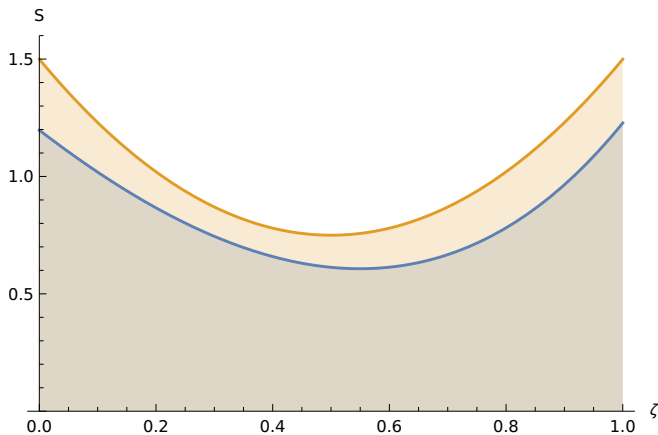


FIG. 3. Rescaled spectra of Compton radiation  $S$  defined in Eq. (8) for an electron energy  $E_e = 16.5$  GeV and an incident laser photon energy of 1 eV (blue curve), compared with the Thomson spectrum (orange curve).  $\zeta = \omega/\omega_{\max}$ . The integral Compton cross section is about 0.81 times the integral Thomson cross section).

The Compton radiation spectrum given by Eq. (6) depends on the energy of the incident laser photon measured in the electron reference frame,  $2\gamma\omega_{\text{las}}$ . The total cross section, Eq. (7), decreases with the energy of the incident laser photon.

### C. Polarization of gammas

As is seen from Fig. 3, for low energies of laser photons  $\epsilon_{\text{las}} \lesssim 10$  eV the spectrum of Compton photons resembles the Thomson spectrum, which has a simple form (see Fig. 4 and [11]):

$$S(\zeta) = \frac{3}{2} [1 - 2\zeta(1 - \zeta)]; \quad 0 \leq \zeta \leq 1, \quad (8)$$

where  $\zeta := \omega/\omega_{\max}$  is the energy of the emitted gamma-ray photon normalized to its maximum. The low-energy end of the spectrum, being of little significance for gamma sources, scales as  $\omega^{\min} \sim \omega_{\text{las}}/2\gamma^2$  and is approximated with zero.

The spectrum described by Eq. (8) may be decomposed into a sum of two sub-spectra with ‘orthogonal’ polarization components, see [12]. For a circular laser polarization, they are  $S_{\text{neg}}$  – the negative polarization constituent with the same polarization as the incident radiation, and  $S_{\text{pos}}$  – the positive constituent with the opposite polarization, see Fig. 4:

$$S_{\text{pos}} = 3\zeta^2/2; \quad S_{\text{neg}} = 3(1 - \zeta)^2/2.$$

The degree of polarization  $\rho$  is defined as

$$\rho(\zeta) := \frac{S_{\text{pos}} - S_{\text{neg}}}{S_{\text{pos}} + S_{\text{neg}}} = \frac{3\zeta}{2 - \zeta + 2\zeta^2}.$$

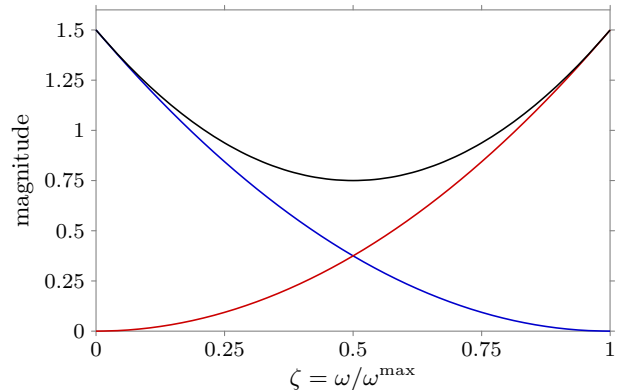


FIG. 4. Thomson photon spectrum (black) and its constituents: ‘positively polarized’ (red) and ‘negatively polarized’ (blue) gamma-ray photons.

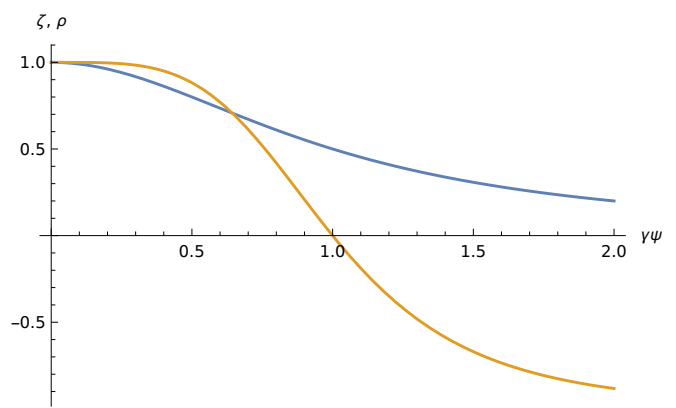


FIG. 5. Relative energy of gamma ray photons (blue curve) and degree of polarization (orange) vs. emission angle.

It should be emphasized that the degree of polarization has probabilistic sense: if, for instance,  $\rho = 0.7$ , one obtains 85% of gamma-ray photons ‘positively polarized’ and 15% ‘negatively polarized’.

The dependence of the degree of polarization  $\rho$  and of the normalized gamma-ray photon energy  $\zeta$  as a function of the emission angle (multiplied by  $\gamma_*$ ) is presented in Fig. 5.

As it can be seen from the figure, at the angle  $\gamma_*\psi = 1$ , the photon energy decreases by half, and the degree of polarization is zero, i.e. positively- and negatively-polarized photons are equal in numbers. Upon further increase of the observation angle, the photon energy continues to drop while the number of negatively polarized photons prevails over the positive ones.

Compton radiation is quasi-monochromatic: if the laser beam is scattered by a zero-emittance electron beam and observed through an angular filter (a pinhole or a mask selecting a narrow ‘ring’ around the radiation axis that matches the electron trajectory), every photon scattered by an electron with a given energy at a definite angle to its trajectory has a fixed energy and degree of

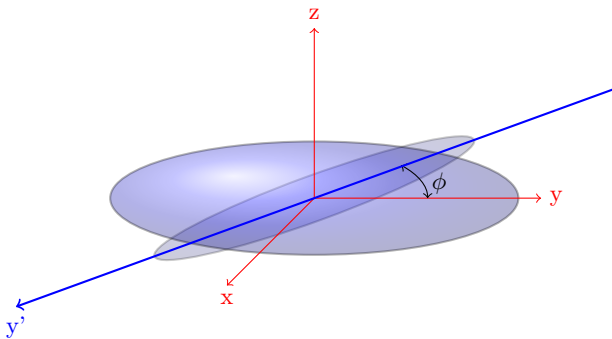


FIG. 6. Scheme of bunch-pulse crossing.

polarization.

In contrast to a single electron or a monoenergetic filament electron beam, realistic electron beams with finite energy spread and emittance, scatter-off radiation with larger spectral bandwidth; at XFELs the contribution of emittance is dominant [12]. In the case of multi-GeV electrons the energy half-maximum angle (zero degree of polarization)  $\psi_{1/2}$  is rather small. For example, for  $E_e = 16.5$  GeV and  $\epsilon = 1$  eV the photon energy is diminished by half at  $\psi_{1/2} \approx 35 \mu\text{rad}$ .

The correlation of the photon degree of polarization with its energy is independent of electron's trajectory direction. A Coincidence scheme for defining the gamma-ray photon energy and polarization through measurement of the electron energy that emitted it is therefore justified.

#### D. Yield of photons

The yield of gamma-ray photons per single crossing of the incident photon pulse with the electron bunch, both assumed having a 3D Gaussian shape [11], reads

$$Y = \frac{N_{\text{pp}} N_e \sigma_C}{2\pi \sqrt{(\sigma_z'^2 + \sigma_z^2) [\sigma_x^2 + \sigma_x'^2 + (\sigma_y^2 + \sigma_y'^2) \tan^2 \frac{\phi}{2}]}} \quad (9)$$

where  $N_{\text{pp}}, N_e$  are populations of the incident radiation pulse and of the bunch, respectively,  $\sigma_{x,y,z}, \sigma'_{x,y,z}$  are their horizontal, longitudinal, and vertical rms dimensions and  $\sigma_C$  is the total Compton cross-section in Eq. (7).

### III. COMPTON SOURCES AT THE EUROPEAN XFEL

Owing to the high density and high energy electron beams needed to drive X-ray FELs, we propose to adapt them as Compton sources of gamma-ray photons in the GeV energy range, e.g., for experiments in Quantum Chromo-Dynamics.

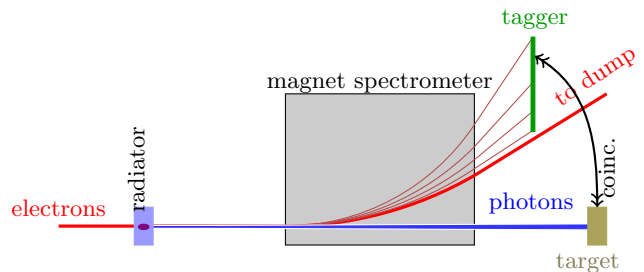


FIG. 7. Scheme of experimental setup.

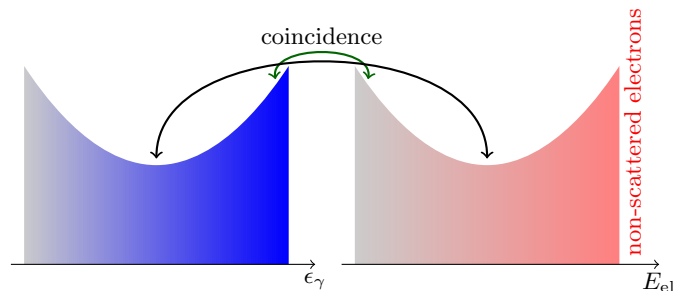


FIG. 8. Relation of the electron's (red) to gamma's (blue) spectra.

Figure 7 presents a scheme of such experimental setup. It is important that the electron spectrum upon interaction with the radiation pulse consists of two distinct parts: the recoiled and the undisturbed fractions. The recoiled fraction is small, less than  $10^{-4}$  of the total.

'Photon tagging' assigns the energy loss of *individual electron* to the energy of the emitted photon in coincidence, as depicted in Fig. 8.

#### A. Radiation source: infrared laser

Below we discuss whether a ten  $\mu\text{A}$  - order average current, deliverable by the accelerator of the European XFEL, is able to produce sufficient flux of scattered GeV photons.

The number of back-scattered photons per crossing is proportional to the populations and a geometrical factor. The latter is inversely proportional to the dimensions of bunch and photon pulse. The bunch population is by three orders of magnitude smaller than that in LEPS (storage ring SPring-8, [3]), but it is compensated by a much larger population of the laser photons stored in resonator. In addition, the small transverse size of low-emittance electron bunches at the European XFEL enhances the yield as well.

The key element of the laser system proposed for the European XFEL is a resonator. The resonator is capable of storing up to 10–20 thousand pulses of 100 Watt infrared laser. The stored energy may reach levels as high as 30 mJ per pulse, [13].

TABLE I. Main parameters of gamma sources.

experiment parameter	LEPS2 (SPring8)	GlueX (CEBAF)	XFEL+laser (European XFEL)
$E_e$ , GeV	8	12	4.0 8.0 11.5 14.0 16.5 17.5
$I_{\text{beam}}$ , A	0.1	$1.5 \times 10^{-7}$	$2.7 \times 10^{-5}$
radiator	lasers	diamond $\Delta = 50 \mu\text{m}$	las+res
$\lambda_{\text{las}}$ , nm	355 266	$\sim 2 \times 0.15$	1064
$\epsilon_\gamma$ , GeV	1.3–2.39 1.6–2.89	8.4–9	0.15–0.23 0.55–0.87 1.09–1.72 1.57–2.47 2.11–3.33 2.62–4.14
$\rho$ , %	$\gtrsim 98$	(35–40)	50–100
$W_{\text{laser}}$ , W	8		$\lesssim 10^6$
flux, phot/s	0.8 10 <sup>6</sup> 10 <sup>5</sup>	10 <sup>7</sup>	$\lesssim 10^9$ <sup>a</sup>

<sup>a</sup> assuming  $10^3$  events per second

The main parameters of the proposed gamma source together with those under construction, LEPS2 [3] and GlueX [4], are listed in Table I. The range of gamma-photon energy for the European XFEL-based source is taken such that the polarization at the bottom edge equals to 1/2:

$$\rho(\zeta_{1/2}) = \frac{1}{2} \Rightarrow \zeta_{1/2} = \frac{3 - \sqrt{3}}{2} \approx 0.63.$$

The polarization is linear for GlueX, while for other projects it is determined by the polarization of laser. Corresponding parameters in each column are marked with the same color.

### B. Capability of XFEL accelerator to produce GeV photons

Comparing the European XFEL accelerator to the storage ring SPring-8, [14], where the GeV-photons Compton source LEPS2 has been built, one can see a 4 orders of magnitude larger current of the electrons circulating in the ring,  $\sim 300$  mA, as compared with  $\sim 10 \mu\text{A}$  in the linac. On the other hand, due to a factor two higher maximum electron energy of the linac (17.5 GeV), the European XFEL could produce four times higher photon energy with the same laser wavelength. Moreover, the quality of the linac beam – in terms of transverse emittances and the bunch length – allows for substantial reduction of the geometric factor [the denominator

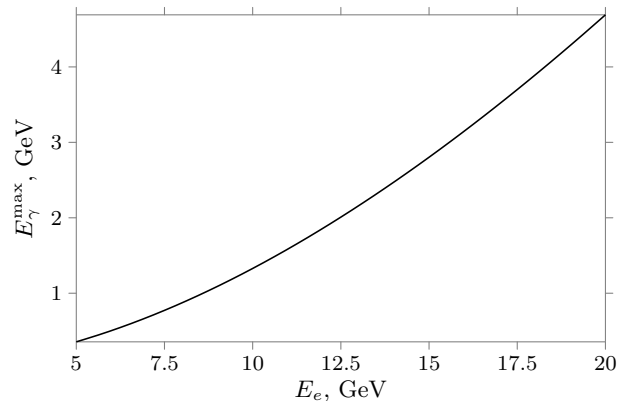


FIG. 9. The gamma-photon maximal energy as a function of the electron energy for  $E_{\text{laser}} = 1$  eV.

in (9)].

Finally, for the realistic case of a moderate but still higher energy than attained in [14], the laser resonator of the kind developed for Compton x-ray sources – see, e.g., [15–17] – and the sources of polarized positrons for ILC and CLIC projects of lepton colliders [18–20] may be employed. The optical resonator is capable of increasing the power of a YAG laser (1  $\mu\text{m}$  wavelength) by  $(2 \dots 4) \times 10^3$  times, see e.g. papers on Compton X-ray compact sources [21, 22].

Making use of the parameters of the European XFEL accelerator [23], we estimated the performance of a Compton source of polarized GeV photons. We took the parameters of a laser system that was considered for the projects of lepton colliders ILC and CLIC. Currently, a similar system is under construction at the IJC laboratory (Orsay, France) for the ThomX Compton source.

The dependency of the maximum energy of photons on the electron energy is presented in Fig.9.

A 16.5 GeV electron beam of the European XFEL, assuming a laser resonator storing 1 mJ laser pulse at 1.164 eV photon energy (providing 8 degrees crossing angle) produces a Compton spectrum with the maximum energy  $\sim 4$  GeV with an efficiency of  $10^{-4}$  photons per electron-crossing. The data from estimations and simulations are listed in Table III B.

Simulations were done with a Monte-Carlo code initially written for study of beam dynamics in Compton storage rings. Spectra of the photon flux are presented in Fig. 10.

Our simulations show that the spectrum is rather uniform, and the fraction of negatively polarized gammas negligible for  $\zeta \gtrsim 0.8$ .

## IV. SUMMARY AND DISCUSSION

Installation of a laser resonator and an electron tagger system at the European XFEL makes it possible to carry out QCD experiments. The energy range of Compton

TABLE II. Simulated parameters of Compton source

parameter	value	units
electron energy	16.5	GeV
bunch charge	1	nC
bunch length	24	$\mu\text{m}$
bunch tr. $\sigma_x/\sigma_z$ at IP	20/20	$\mu\text{m}$
energy of photon	1.164	eV
pulse energy	1	mJ
pulse trans. $\sigma'_x/\sigma'_z$ at IP	20/20	$\mu\text{m}$
pulse long. $\sigma'_y$ at IP	50	$\mu\text{m}$
crossing angle	8	deg
max. gammas energy	3.88	GeV
half max angle $\psi_{1/2}$	35	$\mu\text{rad}$
yield per crossing	$3.5 \times 10^4$	gammas

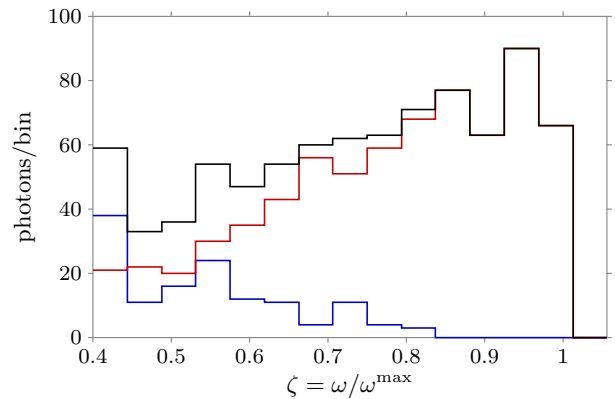


FIG. 10. Simulated photon spectrum (black) and its constituents: ‘positively polarized gammas’ (red) and ‘negatively polarized’ (blue). 16.5 GeV electrons crossed by 1.164 eV laser at 8 deg.

backscattered gamma-ray photons, their flux and polarization are in range with those at experimental setups under construction and fill the ‘energy gap’ between the most modern experimental setups .

Realization of the proposal would be a “stepping stone” to LUXE project [7] dedicated to the study of interaction between relativistic electrons with powerful laser pulses.

## ACKNOWLEDGMENTS

Authors would like to thank Serguei Molodtsov for his interest and support. Computations were done with help of WOLFRAM MATHEMATICA CLOUD package [24], provided to one of coauthors (EB).

- 
- [1] M. Nakatsutsumi, K. Appel, G. Priebe, I. Thorpe, A. Pelka, B. Muller, and T. Tschentscher, *Scientific Instrument High Energy Density Physics (HED)*, Technical design report XFEL.EU TR-2014-001 (European XFEL, 2014).
- [2] T. Barklow, C. Emma, Z. Huang, A. Naji, E. Nanni, A. Schwartzman, S. Tantawi, and G. White, XCC: an X-ray FEL-based  $\gamma\gamma$  Compton collider Higgs factory, <https://arxiv.org/abs/2306.10057> (2023).
- [3] N. Muramatsu, M. Yosoi, T. Yorita, Y. Ohashi, *et al.*, SPring-8 LEPS2 beamline: A facility to produce a multi-GeV photon beam via laser Compton scattering, *NIM A* **1033**, 166677 (2022).
- [4] S. Adhikari, C. Akondi, H. Al Ghouli, A. Ali, *et al.*, The GlueX beamline and detector, *NIM A* **987**, 164807 (2021).
- [5] A. D’Angelo, O. Bartalini, V. Bellini, P. Sandri, D. Moricciani, L. Nicoletti, and A. Zucchiatti, Generation of Compton backscattering  $\gamma$ -ray beams, *Nucl. Instrum. Meth.A* **455**, 1 (2000), proceedings of the Int. Symp. on New Visions in Laser-Beam.
- [6] T. Heinzl and A. Ilderton, Corrections to laser electron Thomson scattering, <https://arxiv.org/abs/1307.0406> (2013).
- [7] H. Abramowicz *et al.*, Conceptual design report for the LUXE experiment, *Eur. Phys. J. Spec. Top.* **230**, 2445 (2021).
- [8] A. Fedotov, A. Ilderton, F. Karbstein, B. King, D. Seipt, H. Taya, and G. Torgrimsson, Advances in QED with intense background fields, <https://arxiv.org/abs/2203.00019v2> (2023).
- [9] F. Arutyunian and V. Tumanian, The Compton effect on relativistic electrons and the possibility of obtaining high energy beams, *Physics Letters* **4**, 176 (1963).
- [10] R. Hajima and M. Fujiwara, Narrow-Band GeV photons generated from an x-ray free-electron laser oscillator, *Phys. Rev. Accel. Beams* **19**, 020702 (2016).
- [11] E. Bulyak and V. Skomorokhov, Parameters of Compton x-ray beams: Total yield and pulse duration, *Phys. Rev. ST Accel. Beams* **8**, 030703 (2005).

- [12] E. Bulyak and J. Urakawa, Spectral properties of Compton inverse radiation: Application of Compton beams, *Journ. of Physics: Conf. Series* **517**, 012001 (2014).
- [13] K. Dupraz, M. Alkadi, M. Alves, L. Amoudry, *et al.*, The ThomX ICS source, *Physics Open* **5**, 100051 (2020).
- [14] N. Muramatsu, M. Yosoi, T. Yorita, Y. Ohashi, *et al.*, SPring-8 LEPS2 beamline: A facility to produce a multi-GeV photon beam via laser Compton scattering, *arXiv: 2112.07832v1* (2021).
- [15] C. Bruni, N. Artemiev, R. Roux, A. Variola, F. Zomer, and A. Loulergue, Thomx: A high flux compact x ray source, *UVX 2010 - 10e Colloque sur les Sources Coherentes et Incoherentes UV, VUV et X: Applications et Developpements Recents* (2011).
- [16] K. Dupraz, M. Alkadi, M. Alves, L. Amoudry, *et al.*, The ThomX ICS source, *Physics Open* **5**, 100051 (2020).
- [17] B. Günther, R. Gradl, C. Jud, E. Eggl, J. Huang, S. Kulpe, K. Achterhold, B. Gleich, M. Dierolf, and F. Pfeiffer, The versatile X-ray beamline of the Munich Compact Light Source: design, instrumentation and applications, *J. Synchrotron Rad.* **27**, 1395 (2020).
- [18] L. Rinolfi, F. Zimmermann, E. Bulyak, P. Gladkikh, A. Kalamaiko, T. Omori, J. Urakawa, and K. Yokoya, 3.5 GeV superconducting stacking ring for Compton based polarized positron source of CLIC (rep tupme056), in *IPAC 2013, Shanghai, China, 13-17 May 2013* (2013).
- [19] J. A. Fernandez *et al.*, A large hadron electron collider at CERN, *Journal of Physics G: Nuclear and Particle Physics* **39** (2015).
- [20] I. Adachi *et al.*, The international linear collider: Report to snowmass 2021, Preprint PUBDB-2022-01473, DESY, Theorie-Gruppe (2022).
- [21] T. Brümmer, S. Bohlen, F. Grüner, *et al.*, Compact all-optical precision-tunable narrowband hard Compton X-ray source, *Scientific Reports* **12(1)**, <https://doi.org/10.1038/s41598-022-20283-8> (2022).
- [22] B. Hornberger, J. Kasahara, R. Ruth, R. Loewen, and J. Khaydarov, Inverse Compton scattering X-ray source for research, industry and medical applications, *Proc. SPIE 11886, XVII International Conference on X-Ray Lasers* (2020) **12(1)**, <https://doi.org/10.1117/12.2591977> (2021).
- [23] X. F. E. L. Collaboration, XFEL accelerator, *xfel.desy.de/.../XFEL-TDR-Ch-4.pdf* (2021).
- [24] Wolfram Research, Inc., *Mathematica, Version 12.0* (2019), Champaign, IL, 2019.